Published in final edited form as:
*J Neurophysiol*. 2001 March ; 85(3): 1088–1096.

# Neonatal Deafferentation Does Not Alter Membrane Properties of Trigeminal Nucleus Principalis Neurons

**Fu-Sun Lo** and **Reha S. Erzurumlu**
Department of Cell Biology and Anatomy, Louisiana State University Health Sciences Center, New Orleans, Louisiana 70112

## Abstract

In the brain stem trigeminal complex of rats and mice, presynaptic afferent arbors and postsynaptic target cells form discrete modules ("barrelettes"), the arrangement of which duplicates the patterned distribution of whiskers and sinus hairs on the ipsilateral snout. Within the barrelette region of the nucleus principalis of the trigeminal nerve (PrV), neurons participating in barrelettes and those with dendritic spans covering multiple barrelettes (interbarrelette neurons) can be identified by their morphological and electrophysiological characteristics as early as postnatal day 1. Barrelette cells have focal dendritic processes, are characterized by a transient $K^+$ conductance ($I_A$), whereas interbarrelette cells with larger soma and extensive dendritic fields characteristically exhibit low-threshold T-type $Ca^{2+}$ spikes (LTS). In this study, we surveyed membrane properties of barrelette and interbarrelette neurons during and after consolidation of barrelettes in the PrV and effects of peripheral deafferentation on these properties. During postnatal development (PND1–13), there were no changes in the resting potential, composition of active conductances and $Na^+$ spikes of both barrelette and interbarrelette cells. The only notable changes were a decline in input resistance and a slight increase in the amplitude of LTS. The infraorbital (IO) branch of the trigeminal nerve provides the sole afferent input source to the whisker pad. IO nerve transection at birth abolishes barrelette formation as well as whisker-related neuronal patterns all the way to the neocortex. Surprisingly this procedure had no effect on membrane properties of PrV neurons. The results of the present study demonstrate that distinct membrane properties of barrelette and interbarrelette cells are maintained even in the absence of input from the whiskers during the critical period of pattern formation.

## Introduction

The patterned array of whisker follicles and sinus hairs on the snout of nocturnal rodents is replicated by the distribution of whisker-specific trigeminal axon arbors and select sets of postsynaptic neurons in several sensory nuclei of brain stem trigeminal complex (BSTC) (Bates and Killackey 1985; Belford and Killackey 1979; Erzurumlu et al. 1980; Ma 1993; Ma and Woolsey 1984). The whisker-specific neuronal modules in the BSTC are referred to as "barrelettes" (Ma and Woolsey 1984). Barrelette neurons of the nucleus principalis of the trigeminal nerve (PrV) convey this pattern to the ventroposteromedial nucleus of the thalamus, where their synaptic partners, the thalamocortical projection cells form the "barreloids," which in turn relay this information to the layer IV granule cells of the primary somatosensory cortex where the "barrels" form (Belford and Killackey 1980; Van der Loos 1976; Van der Loos and Woolsey 1973). Barrelette formation in the BSTC begins shortly before birth and is consolidated by postnatal day (PND) 5 (Belford and Killackey 1980;



Address for reprint requests: F.-S. Lo, Dept. of Cell Biology and Anatomy, Louisiana State University Medical Center, 1901 Perdido St., New Orleans, LA 70112 (flo@lsuhsc.edu).

Chiaia et al. 1992; Erzurumlu and Killackey 1983; Ma 1993; O'Leary et al. 1994; Woolsey 1990). Many lines of evidence indicate that central whisker-related patterns depend on an intact sensory periphery during a critical period in development (Bates et al. 1982; Belford and Killackey 1980; Durham and Woolsey 1984), and more recent studies indicate that patterning of neural elements is mediated via *N*-methyl-$_D$-aspartate (NMDA) receptors (Iwasato et al. 1997, 2000; Kutsuwada et al. 1996; Li et al. 1994). Disruptions of the sensory periphery before PND 3–4 irreversibly alter the development and maintenance of whisker-specific central neural patterns (see Erzurumlu and Killackey 1982; Jhaveri and Erzurumlu 1992; O'Leary et al. 1994; Woolsey 1990 for reviews). In mice with targeted mutations of the critical subunit of the NMDA receptor, these patterns fail to develop (Iwasato et al. 1997; Li et al. 1994).

Previous morphological studies showed that the barrelette region of the PrV contains three types of cells: barrelette, interbarrelette, and GABAergic cells (Ginestal and Matute 1993; Ma 1991, 1993). Barrelette cells have dendritic trees confined to a single barrelette (Arends and Jacquin 1993) and project to the thalamus (Erzurumlu et al. 1980). Interbarrelette cells have dendritic trees spanning several barrelettes and contribute internuclear connections within the BSTC (Jacquin et al. 1990; Nasution and Shigenaga 1987). GABAergic cells participate in local inhibitory circuits. Recently we reported that in the PrV, barrelette, and interbarrelette neurons can be distinguished by their electrophysiological properties and morphological features (Lo et al. 1999). By using whole cell patch recording, immuno-histochemistry, and intracellular biocytin staining techniques, we showed that barrelette cells receive excitatory inputs from one whisker and a strong lateral inhibition from neighboring whiskers. Interbarrelette cells receive excitatory inputs from multiple sources and a weak lateral inhibition. In both types of cells, the excitation is mediated by both NMDA and non-NMDA receptors, whereas the inhibition is exclusively mediated by $GABA_A$ receptors. Specific electrophysiological properties of barrelette neurons undoubtedly play a role in transfer of “pattern”-related information from incoming trigeminal afferents to barrelette cells or conveying this information to upstream trigeminal centers such as the dorsal thalamus (Erzurumlu and Guido 1996). In the first part of the present study, we investigated developmental changes in membrane properties of neurons in the barrelette region of PrV of neonatal rats (PND1–13). As early as at PND 1, PrV neurons can be electrophysiologically identified as barrelette and inter-barrelette cells. The barrelette cell is characterized by a prominent transient $K^+$ conductance ($I_A$), whereas the interbarrelette cell, by a low-threshold T-type $Ca^{2+}$ spike (LTS). During postnatal development from PND 1 to 13, there are no changes in resting potential, composition of active conductances, and $Na^+$ spike of both barrelette and interbarrelette cells except a decline of input resistance and a slight increase in amplitude of the LTS. These observations suggest that membrane properties of PrV neurons are well developed at birth.

The infraorbital (IO) branch of the trigeminal nerve carries all the information from the whiskers and sinus hairs to the BSTC and if sectioned or partially damaged during the first few days after birth, related central patterns are completely or partially abolished in a predictable fashion (e.g., see Bates and Killackey 1985; Belford and Killackey 1979, 1980; Durham and Woolsey 1984; Yip et al. 1987). In the second part of the present study, we examined whether peripheral deafferentation affects membrane properties of PrV neurons in the barrelette region. Surprisingly, the membrane properties of PrV neurons after denervation were indistinguishable from those with an intact IO nerve up to a week after nerve transection.

# Methods

## Brain slice preparation

Sprague-Dawley rat pups ranging in age from PND 1 to 13 were deeply anesthetized with fluothane (Halothane) and then killed by decapitation. The brain was removed and immersed in cold (4°C), sucrose-based artificial cerebrospinal fluid [ACSF, containing (in mM): 234 sucrose, 2.5 KCl, 1.25 $NaH_2PO_4$, 10 $MgSO_4$, 24 $NaHCO_3$, 11 glucose, and 0.5 $CaCl_2$ bubbled with 95% $O_2$-5% $CO_2$ (pH = 7.4)]. The brain stem was embedded in 2% agar and cut into 500-$\mu$m-thick transverse sections with a vibratome (Electron Microscopy Sciences). Slices containing the PrV were placed in a submerged-type recording chamber (Fine Science Tools) and continuously perfused (2 ml/min) with normal ACSF [containing (in mM) 124 NaCl, 2.5 KCl, 1.25 $NaH_2PO_4$, 2 $MgSO_4$, 26 $NaHCO_3$, 10 glucose, and 2 $CaCl_2$, pH = 7.4] at room temperature.

## Electrophysiological methods

Recordings began ≥1 h after incubation in normal ACSF. Whole cell patch micropipettes were pulled horizontally in two stages from borosilicate glass (WPI, K150F-4) with a P-87 puller (Sutter Instrument). The patch electrodes were backfilled with a potassium-based solution [containing (in mM) 140 K-Gluconate, 10 HEPES, 1.1 EGTA-Na, 0.1 $CaCl_2$, 2 $MgCl_2$, 2 ATP-Na, and 0.2 GTP-Na, pH = 7.25] with a tip resistance of 7–10 MΩ. Neurons in the ventral part of the PrV (barrelette region) were blindly patched with the techniques described by Blanton et al. (1989) and Ferster and Jagadeesh (1992). In brief, patch-electrode resistance was monitored in Bridge Mode of Axoclamp 2B amplifier by measuring the voltage drop induced by a current pulse (−100 pA, 200 ms). An increase in resistance of 20–50 MΩ was taken as a sign that the tip of the electrode contacted the surface of a neuron. A steady negative pressure was applied with a 5-ml syringe to form a gigaohm seal. Then a brief suction was used to break into the neuronal soma. The formation of whole cell configuration was indicated by a sudden drop in seal resistance and a DC drop of >55 mV. After “break-in,” the serial resistance was completely compensated with bridge balance, and junction potential (Neher 1992) was not corrected. We only collected data from cells with resting membrane potential negative to −55 mV and input resistance >200 MΩ with an Instrutek VR10B interface unit and stored on a Macintosh Power PC (9500/132) with *Pulses* (HEKA) software program.

Input resistance of recorded neurons was determined by the voltage drop induced by a small negative current pulses (−10 pA, 200 ms) at resting potential. Different DC pulse protocols were used to induce active conductances of trigeminal neurons. The identification of various active conductances was based on their voltage dependency and pharmacology. For example, the transient $K^+$ conductance ($I_A$) was specifically blocked by 1 mM 4-aminopyradine (4-AP), the hyperpolarization-activated H conductance was blocked by 1 mM $CsCl_2$, and the low-threshold $Ca^{2+}$ T-type conductance was blocked by 200 $\mu$M $NiCl_2$. To compare voltage-dependent conductances among different cells, the membrane potential was held at −60 mV except in cases where indicated.

For biocytin-labeling experiments, we filled the patch electrodes with 1% biocytin dissolved in potassium-based solution. Once membrane properties and synaptic responses were characterized, the cells were filled intracellularly with biocytin by passing AC pulses (± 1 nA, 60 ms for each cycle, 100 cycles) through the biocytin-filled recording electrode.

## IO nerve transection

In a separate set of experiments, PND 0 pups were anesthetized, and a unilateral incision was made caudal to the whisker pad. The IO nerve can be visualized under the skin and

connective tissues as it emerges from the infraorbital foramen. The nerve was then cut with sterile microscissors just between the eye and the caudal edge of the whisker pad. The wound was sutured, and the pup allowed to recover from anesthesia. The lesions were made unilaterally, therefore allowing for direct comparisons in brain stem slices between the lesioned and unoperated sides. Once the pups recovered from anesthesia, they were returned to the home cage with their mother. At PND 4–8, these pups were killed by an overdose of Fluothane, and the brain stems were dissected out after decapitation. The brain stems were rinsed in ACSF with sucrose and sectioned into slices as described in the preceding text for recordings. In each case, the lesioned and normal sides were marked. Whole cell recordings were then performed in the ventral (barrelette) part of the PrV.

### Histological methods

One hour after biocytin injection, the slice was fixed by 4% paraformaldehyde in 0.1 M phosphate buffer for 48 h. The fixed slice was transferred into phosphate-buffered saline (PBS) at 4°C and then incubated in 10% methanol +3% $H_2O_2$ overnight. After several rinses in PBS, the slice was reacted with avidin-biotin complex (ABC Elite kit, Vector Laboratories) overnight at 4°C (1:100 in PBS with 1.8% NaCl and 0.5% Triton X-100). Next day, the slice was rinsed again in PBS and 0.1 M acetate buffer (pH = 6.0) and incubated in glucose oxidase-nickel ammonium sulfate and diaminobenzidine until the labeled cells could be visualized. The slice was rinsed in acetate buffer and PBS, mounted on to a slide, dehydrated, and cover slipped. Labeled cells were drawn with a drawing tube attached to a Nikon Labophot microscope.

For denervation experiments, cytochrome oxidase histochemistry (Wong-Riley and Welt 1980) was used as an anatomical marker for barrelettes at PND5. Briefly, the rat pups were overdosed with pentobarbital sodium and perfused transcardially with PBS followed by 4% paraformaldehyde in 0.1 M phosphate buffer (pH = 7.4). After overnight fixation at 4°C, the brains were transferred to 30% sucrose in phosphate buffer at 4°C for cryoprotection. The brain stem was sectioned frozen in the coronal plane at a thickness of 75 $\mu$m. Sections were incubated in a solution of 90 ml PBS, 40 mg cytochrome C, 10 mg diaminobenzidine and 4 g sucrose at 37°C until they turned golden brown. At this point, the reaction was stopped by several rinses in PBS, mounted on to glass slides, and coverslipped with a glycerol-based mounting medium. Photomicrographs from these sections were taken using Coolsnap computerized imaging system. The figures were made with the use of ADOBE Photoshop 4 program. No alterations were made in the images except for adjustments of brightness and contrast.

## Results

### Physiological identification of barrelette and interbarrelette cells

We recorded voltage responses to intracellular current pulses from 77 neurons in the barrelette region of PrV of normal neonatal rats (PDN 1–13) and 15 neurons from denervated rats. Barrelette neurons showed a transient $K^+$ conductance ($I_A$) and a hyperpolarization-acitvated mixed cation conductance ($I_H$). These cells were further identified as barrelette neurons by intracellular biocytin labeling (Fig. 1A) (also see Lo et al. 1999). Membrane hyperpolarization from resting potential resulted in a “depolarizing sag” (Fig. 1, B and C, indicated by H) that was blocked by $Cs^{2+}$ (see also Lo et al. 1999). On the cessation of current pulses, the repolarization of membrane potential was delayed by a hyperpolarizing tail (indicated by A in Fig. 1B). Depolarization from a hyperpolarizing state exhibited a hyperpolarizing notch (indicated by A in Fig. 1C) that delayed the generation of $Na^+$ spikes. The notch was blocked by application of 4-AP (Lo et al. 1999).

Interbarrelette neurons possess a prominent LTS mediated by T-type $Ca^{2+}$ channels and an H conductance. Intracellular biocytin labeling shows that these cells have long dendritic trees that span multiple barrelette territories (Fig. 1D) (also see Arends and Jacquin 1993; Lo et al. 1999). In these neurons, membrane hyperpolarization also caused a depolarizing sag (Fig. 1, E and F, indicated by H). Repolarization (Fig. 1E) or depolarization (Fig. 1F and F) from hyperpolarizing state induced a triangular LTS (Fig. 1, E, indicated by T) that proved to be mediated by T-type $Ca^{2+}$ channels (Lo et al. 1999). We next surveyed developmental changes in membrane properties of barrelette and interbarrelette cells and followed peripheral denervation as described in the following text.

## Resting membrane potential of barrelette and interbarrelette neurons during postnatal development

Scatter plots of resting membrane potentials of both barrelette and interbarrelette neurons (Fig. 2A) exhibited little changes between PND 1 and 13. The values for barrelette (●, $n$ = 49) and interbarrelette cells ((○, $n$ = 28) intermingled at all postnatal ages. We arbitrarily divided animals into three age groups: PND 1–3 (sensitive period, during which whisker-specific patterns can be altered by whisker lesions or IO nerve damage), PND 4–6 (consolidation period, during which whisker-specific patterns are consolidated and are no longer subject to structural changes following whisker lesions or IO nerve damage), and PND 7–13 (mature, adult-like period). The averaged resting potentials of barrelette cells were −60.0 ± 1.20 mV ($n$ = 10) at PND 1–3, −63.1 ± 1.16 mV ($n$ = 20) at PND 4–6, and −61.3 ± 0.48 mV ($n$ = 19) at PND 7–13. There was no significant difference ($P$ > 0.05) in the averaged resting potentials among the three different age groups (Fig. 2B). The averaged resting potentials of interbarrelette cells were − 61.2 ± 1.29 mV ($n$ = 7) at PND 1–3, −60.1 ± 1.04 mV ($n$ = 12) at PND 4–6, and −60.3 ± 1.13 mV ($n$ = 9) at PND 7–13. There was no difference in resting membrane potential ($P$ > 0.05) during postnatal development either. Furthermore there was no difference ($P$ > 0.05) between barrelette and interbarrelette cells at each age group examined. Therefore resting membrane potential for both barrelette and interbarrelette cells at birth are similar to those seen 2 wk later when the pups have already begun whisking behavior.

## Decrease in input resistance during postnatal development

Scatter plotting of input resistances of barrelette and interbarrelette neurons (Fig. 2C) suggested a decrease in input resistance during postnatal development. For barrelette cells, the mean input resistance at PND 1–3 (742.9 ± 86.7 MΩ) was similar to that at PND 4–6 (749.8 ± 47.9 MΩ, $P$ > 0.05). However, the mean input resistance at PND 7–13 (519.0 ± 43.8 MΩ) was significantly lower than that at PND 1–3 ($P$ < 0.02, Fig. 2D,**). The mean input resistance of interbarrelette cells was 659.6 ± 111.9 MΩ at PND 1–3, then it declined to 488.0 ± 55.4 MΩ at PND 4–6 and finally to 346.1 ± 37.5 MΩ at PND 7–13, which was significantly smaller than seen at PND 1–3 ($P$ < 0.02, Fig. 2D, **). The decline of input resistance for interbarrelette cells appeared earlier than for barrelette cells, suggesting that interbarrelette cells may develop faster than barrelette cells. At PND 1–3, there was no difference in averaged input resistance between barrelette cells and interbarrelette cells ($P$ > 0.05). However, at PND 4–6 and 7–13, the input resistance of interbarrelette cells was significantly smaller ($P$ < 0.02) than that of barelette cells (Fig. 2D, ##). This also suggests that postnatal growth of interbarrelette cells is more prominent than barrelette cells.

## Development of active conductances

During postnatal development, active conductances of barrelette cells ($n$ = 49) did not change noticeably. At PND 1–3, barrelette cells possessed A and H conductances and $Na^+$ spikes (Fig. 3A) with similar characteristics observed at PND 4–6 (Fig. 3C) and at PND 7–13 (Fig. 3E), suggesting that active conductances of barrelette cells are fully developed at

birth. In interbarrelette cells, the LTS was already present at PND 1–3 (Fig. 3B). However, the amplitude of LTS slightly increased during development (Fig. 3, D and F) as shown by the scatter plot of LTS amplitudes (Fig. 4A). The mean amplitude of LTS at PND 7–13 (15.2 ± 1.4 mV) was ~48% larger ($P < 0.05$) than that at PND 1–3 (10.7 ± 1.1 mV, Fig. 4B). In addition, the duration of LTS appeared to get shorter in older PrV neurons (Fig. 3, B, D, and F). Since we did not apply $K^+$; channel blockers in the present study, we could not tell if the shortening was caused by a change in kinetics of $Ca^{2+}$ channels or by an increase in $K^+$; conductance. Nevertheless the number of $Na^+$ spikes that superimposed on the LTS decreased during development (Fig. 4, C and D).

### Denervation abolishes patterning of PrV neurons into barrelettes but does not affect their membrane properties

Cytochrome oxidase (CO) or succinic dehydrogenase (SDH) histochemistry are reliable markers that reveal whisker-specific patterns formed by presynaptic terminals and their postsynaptic targets at various stations along the trigeminal neuraxis (Belford and Killackey 1980; Yip et al. 1987). Following IO nerve transection at birth, CO staining showed absence of whisker-specific patterns in the BSTC on the denervated side by PND5 (Fig. 5). We recorded 15 neurons from the ventral part (equivalent barrelette region of normal animals) of the denervated PrV at PND 4–8. All recorded neurons could also be classified as “barrelette” or “interbarrelette” neurons by their electrophysiological properties. The resting membrane potentials and input resistances of “barrelette” cells were plotted together with barrelette cells of normal rats, and there were no differences between the two groups (Fig. 6, A and C). Similarly “interbarrelette” cells on the denervated side had resting potentials and input resistances indistinguishable from the undamaged side (Fig. 6, B and D). In summary, early peripheral denervation, which alters the organization of barrelettes and consequently barreloids and barrels, did not change the resting potential and developmental decrease in input resistance of neurons in PrV. Active conductances of PrV neurons of denervated rats were similar to those of normal rats. As shown in Fig. 7, “barrelette” cells exhibited prominent A and H conductances (Fig. 7, A and B), whereas “interbarrelette” cells showed T and H conductances (Fig. 7, C and D).

## Discussion

Using whole cell recording and biocytin-labeling techniques, we have studied membrane properties of neurons in the barrelette region of PrV in neonatal rats (PND 1–13). Morphologically identified barrelette cells are characterized by a transient $K^+$ conductance ($I_A$), whereas interbarrelette cells by a low-threshold $Ca^{2+}$ conductance ($I_T$). During postnatal development, the resting potential, composition of active conductances, and $Na^+$ spike remain unchanged. The main changes are a decrease in input resistance and a slight increase in amplitude of LTS. Denervation by cutting infraorbital nerve at birth abolishes barrelettes in PrV but does not affect passive membrane properties, composition of active conductances, and $Na^+$ spikes. Therefore membrane properties of PrV neurons are well developed at birth and are not regulated by afferent input from the whiskers during early postnatal days.

### Functional significance of active conductances of barrelette and interbarrelette cells

From PND 1 to 13, all barrelette cells show a transient $K^+$ conductance ($I_A$), whereas all interbarrelette cells show a low-threshold $Ca^{2+}$ conductance ($I_T$). Therefore the two conductances may be considered as physiological signatures of the two types of cells. Because we have not recorded from GABAergic neurons in PrV, we do not know if they have class-specific conductances.

Our preliminary voltage-clamp results from barrelette cells demonstrate that A-type $K^+$ channels are largely inactivated at resting potential (data not shown). Thus $I_A$ may not contribute much to the resting potential of barrelette cells. The function of $I_A$ is likely to modulate the inhibitory postsynaptic potential (IPSP) in barrelette cells. Trigeminal inputs induce a long-lasting IPSP in barrelette cells even at PND 1 (Erzurumlu and Lo 1999; Lo et al. 1999). The hyperpolarization caused by the IPSP may deinactivate A-type channels. Therefore when the IPSP is repolarized, A-type channels are activated so that the IPSP is prolonged and the rebound spike at the end of the IPSP is delayed. Meanwhile the IPSP may also activate H conductance, which curtails the IPSP and enhances the rebound excitation. Thus the IPSP in barrelette cells could be dynamically controlled by these two conductances. The IPSP in barrelette cells is mediated by both feedforward and lateral inhibitory circuits (Lo et al. 1999). The lateral inhibition from surrounding whiskers sharpens the receptive field, whereas the feedforward inhibition curtails postsynaptic excitation. Thus barrelette cells in PrV transmit peripheral vibrissal signals to the thalamus with a sharpened receptive field and phasic temporal properties. Another function of the IPSP is to counteract NMDA receptor-mediated excitatory postsynaptic potential (EPSP) (Lo et al. 1999; Ramoa and McCormick 1994b). A change in the IPSP may secondarily regulate $Ca^{2+}$ influx through NMDA receptors. The activity of NMDA receptors plays a critical role in whisker-specific pattern formation in the rodent BSTC (Iwasato et al. 1997; Kutsuwada et al. 1996; Li et al. 1994). Present results suggest that activity of NMDA receptors may also be regulated by $I_A$ and $I_H$ through their control on the IPSP.

Interbarrelette cells receive excitatory inputs from multiple sources and probably represent the activation level of PrV (Lo et al. 1999). Since interbarrelette cells connect to other subnuclei of the BSTC (Jacquin et al. 1990; Nasution and Shigenaga 1987), their function is probably to coordinate the activity of different brain stem trigeminal subnuclei. Interbarrelette cells have both $I_T$ and $I_H$. These conductances are attributable to the generation of rhythmic bursting activity (Luthi and McCormick 1998; Soltesz et al. 1991; Steriade et al. 1993). Such activity has been observed on “bursting neurons” of gerbil PrV, which are similar to our interbarrelette cells (Sandler et al. 1998). Therefore the bursting activity of interbarrelette cells may enhance coding efficiency and reliability for trigeminal information as also observed in the lateral geniculate nucleus (Reinagel et al. 1999).

## Membrane properties of neurons during development

Postnatal development of membrane properties has been studied in a variety of brain structures, such as the neocortex (Annis et al. 1993; Hugenard et al. 1988; Kang et al. 1996; Kasper et al. 1994; McCormick and Prince 1987; Zhou and Hablitz 1996), hippocampus (Spigelman et al. 1992), striatum (Cepeda et al. 1991), thalamic nuclei (MacLeod et al. 1997; Perez Velazquez and Carlen 1996; Pirchio et al. 1997; Remoa and McCormick 1994a; Tennigkeit et al. 1998; Warren and Jones 1997), cranial nerve nuclei (Bao et al. 1995; Berger et al. 1995, 1996; Kandler and Friauf 1995; Nunez-Abades et al. 1993; Tsuzuki et al. 1995; Viana et al. 1994; Vincent and Tell 1999), cerebellum (Groul et al. 1992; Molnar 1999), spinal cord (Cameron et al. 1991; Gao and Ziskind-Conhaim 1998; Martin-Caraballo and Greer 1999), peripheral ganglia (Donnelly 1999), and retina (Rothe et al. 1999; Wang et al. 1997). Generally, a decline of input resistance has been observed in most of the tested structures, and this may reflect the growth of neurons after birth. An increase (more negative) in resting membrane potential is also observed in most forebrain structures and cerebellar Purkinje cells. This is probably caused by an increase of $Na^+$, $K^+$ pump density (Molnar et al. 1999).

Most tested cranial nerve nuclei neurons do not exhibit developmental changes in resting potential and $Na^+$ spike amplitude, but they do show a decrease in input resistance and $Na^+$ spike duration. The PrV cells we recorded from also fall into this category, except they

demonstrate an unchanged $Na^+$ spike duration. Interestingly, within the BSTC, neurons of the subnucleus interpolaris of the spinal trigeminal nucleus (SPI), show a dramatic increase in $Na^+$ spike amplitude (Guido et al. 1998). In contrast to PrV, SPI exhibits an up-regulation of H conductance and a late emergence of A-type $K^+$ conductance (Guido et al. 1998). These differences between PrV and SPI neurons may be related to their different morphologies and projection patterns. In both the present study and the former study, development of electrophysiological properties of PrV and SPI neurons were studied after birth. It would be interesting to see if there are any changes that occur during late embryonic development during which whisker-specific patterning within the BSTC begins to form (Chiaia et al. 1992).

### Development of membrane properties independent of afferent input

Denervation by cutting the infraorbital nerve at birth abolishes barrelettes in PrV, but membrane properties of PrV neurons are not different from normal animals, suggesting that the development of membrane properties in PrV does not depend on normal synaptic input. This result agrees with the observation on somatosensory cortex in which the development of $Na^+$ spike waveform is independent of synaptic afferents from other structures (Annis et al. 1993). Thus it is still an open question whether membrane properties contribute to pattern formation and its maintenance in the rodent somatosensory pathway. In future studies, it would be of interest to see whether membrane properties of brain stem trigeminal neurons are altered in mice with targeted deletion of the NR1 subunit of the NMDA receptors (Li et al. 1994) or in mice with transgenically lowered levels of NMDA receptor function (Iwasato et al. 1997), as both phenotypes lacking barrelettes in the PrV.

## Acknowledgments

We thank A. Haeberle for help with histology and preparation of figures.

This project was supported by National Institute of Neurological Disorders and Stroke Grant NS-37070 to R. S. Erzurumlu.

## References

Al-Ghoul WM, Miller MW. Development of principal sensory nucleus of the trigeminal nerve of the rat and evidence for a transient synaptic field in the trigeminal sensory tract. J Comp Neurol. 1993; 330:476–490. [PubMed: 8391550]

Annis CM, Robertson RT, O'Dowd DK. Aspects of early postnatal development of cortical neurons that proceed independently of normally present extrinsic influences. J Neurobiol. 1993; 24:1460–1480. [PubMed: 8283185]

Arends JA, Jacquin MF. Lucifer yellow staining in fixed brain slices: optimal methods and compatibility with somatotopic markers in neonatal brain. J Neurosci Methods. 1993; 50:321–339. [PubMed: 8152243]

Bao H, Bradley RM, Mistretta CM. Development of intrinsic electrophysiological properties in neurons from the gustatory region of rat nucleus of solitary tract. Brain Res Dev Brain Res. 1995; 86:143–154.

Bates CA, Erzurumlu RS, Killackey HP. Central correlates of peripheral pattern alterations in the trigeminal system of the rat. III. Neurons of the principal sensory nucleus. Brain Res. 1982; 281:108–113. [PubMed: 7139338]

Bates CA, Killackey HP. The organization of the neonatal rat's brainstem trigeminal complex and its role in the formation of central trigeminal patterns. J Comp Neurol. 1985; 240:265–287. [PubMed: 2999198]

Belford GR, Killackey HP. Vibrissae representation in subcortical trigeminal centers of the neonatal rat. J Comp Neurol. 1979; 183:305–322. [PubMed: 762261]

Belford GR, Killackey HP. The sensitive period in the development of the trigeminal system of the neonate rat. J Comp Neurol. 1980; 193:335–350. [PubMed: 7440771]

Berger AJ, Bayliss DA, Bellingham MC, Umemiya M, Viana F. Postnatal development of hypoglossal motoneuron intrinsic properties. Adv Exp Med Biol. 1995; 381:63–71. [PubMed: 8867824]

Berger AJ, Bayliss DA, Viana F. Development of hypoglossal motoneurons. J Appl Physiol. 1996; 81:1039–1048. [PubMed: 8889732]

Blanton MG, Turco JJL, Kriegstein AR. Whole cell recording from neurons in slices of reptilian and mammalian cerebral cortex. J Neurosci Methods. 1989; 30:203–210. [PubMed: 2607782]

Cameron WE, Jodkowski JS, Fang H, Guthrie RD. Electrophysiological properties of developing phrenic motoneurons in the cat. J Neurophysiol. 1991; 65:671–679. [PubMed: 2051200]

Cepeda C, Walsh JP, Buchwals NA, Levine MS. Neurophysiological maturation of cat caudate neurons: evidence from in vitro studies. Synapse. 1991; 7:278–290. [PubMed: 2042110]

Chiaia NL, Bennett-Clarke CA, Eck M, White FA, Crissman RS, Rhoades RW. Evidence for prenatal competition among the central arbors of trigeminal primary afferent neurons. J Neurosci. 1992; 12:62–76. [PubMed: 1309577]

Donnelly DF. Developmental changes in membrane properties of chemoreceptor afferent neurons of the rat petrosal ganglia. J Neurophysiol. 1999; 82:209–215. [PubMed: 10400949]

Durham D, Woolsey TA. Effects on neonatal whisker lesions on mouse central trigeminal pathways. J Comp Neurol. 1984; 233:424–447. [PubMed: 6707253]

Erzurumlu RS, Bates CA, Killackey HP. Differential organization of the thalamic projection cells in the brainstem trigeminal complex of the rat. Brain Res. 1980; 193:427–433. [PubMed: 7388601]

Erzurumlu, RS.; Guido, W. Cellular mechanisms underlying the formation of orderly connections in developing sensory pathways. In: Mize, RR.; Erzurumlu, RS., editors. Progress in Brain Research Neural Development and Plasticity. Vol. 108. Amsterdam: Elsevier; 1996. p. 287-301.

Erzurumlu RS, Killackey HP. Defining critical and sensitive periods in neurobiology. Curr Top Dev Biol. 1982; 17:207–240. [PubMed: 7140347]

Erzurumlu RS, Killackey HP. Development of order in the rat trigeminal system. J Comp Neurol. 1983; 213:365–380. [PubMed: 6601119]

Erzurumlu RS, Lo FS. Electrophysiological properties and synaptic responses of rat principal sensory nucleus cells during development and following denervation. Soc Neurosci Abstr. 1999; 25:222.

Ferster D, Jagadeesh B. EPSP-IPSP interactions in cat visual cortex studied with in vivo whole-cell patch recording. J Neurosci. 1992; 12:1262–1274. [PubMed: 1556595]

Gao BX, Ziskind-Conhaim L. Development of ionic currents underlying changes in action potential waveforms in rat spinal motoneurons. J Neurophysiol. 1998; 80:3047–3061. [PubMed: 9862905]

Ginestal E, Matute C. Gamma-aminobutyric acid-immunoreactive neurons in the rat trigeminal nuclei. Histochemistry. 1993; 99:49–55. [PubMed: 8468194]

Groul DL, Deal CR, Yool AJ. Developmental changes in calcium conductances contribute to the physiological maturation of cerebellar Purkinje neurons in culture. J Neurosci. 1992; 12:2838–2848. [PubMed: 1377238]

Guido W, Gunhan-Agar E, Erzurumlu RS. Developmental changes in the electrophysiological properties of brain stem trigeminal neurons during pattern (barrelette) formation. J Neurophysiol. 1998; 79:1295–1306. [PubMed: 9497411]

Huguenard JR, Hamill OP, Prince DA. Developmental changes in $Na^+$ conductances in rat neocortical neurons: appearance of a slowly inactivating component. J Neurophysiol. 1988; 59:778–795. [PubMed: 2452862]

Iwasato T, Datwani A, Wolf AM, Nishiyaama H, Taguchi Y, Tonegawa S, Knopfel T, Erzurumlu RS, Itohara S. Cortex-restricted disruption of NMDAR1 impairs neuronal patterns in the barrel cortex. Nature. 2000; 406:726–731. [PubMed: 10963597]

Iwasato T, Erzurumlu RS, Huerto PT, Chen DF, Sasaoka T, Ulupina RE, Tonegawa S. NMDA receptor-dependent refinement of somatotopic maps. Neuron. 1997; 19:1–20. [PubMed: 9247258]

Jacquin MF, Chiaia NL, Haring JH, Rhoades RW. Intersubnuclear connections within the rat trigeminal brainstem complex. Somatosens Mot Res. 1990; 7:399–420. [PubMed: 2291376]

Jhaveri, S.; Erzurumlu, RS. Two phases of pattern formation in the developing rat trigeminal system. In: Sharma, SC.; Goffinet, AM., editors. Development of the CNS in Vertebrates. New York: Plenum; 1992. p. 167-178.

Kandler K, Friauf E. Development of electrical membrane properties and discharge characteristics of superior olivary complex neurons in fetal and postnatal rats. Eur J Neurosci. 1995; 7:1773–1790. [PubMed: 7582130]

Kang J, Huguenard JR, Prince DA. Development of BK channels in neocortical pyramidal neurons. J Neurophysiol. 1996; 76:188–198. [PubMed: 8836218]

Kasper EM, Larkman AU, Lubke J, Blakemore C. Pyramidal neurons in layer 5 of the rat visual cortex. II. Development of electrophysiological properties. J Comp Neurol. 1994; 339:475–494. [PubMed: 8144742]

Kutsuwada T, Sakimura K, Menabe T, Takayama C, Katakura N, Kushiya E, Natsume R, Watanabe M, Inoue Y, Yagi T, Aizawa S, Arakawa M, Takahashi T, Nakamura Y, Mori H, Mishina M. Impairment of suckling response, trigeminal neuronal pattern formation, and hippocampal LTD in NMDA e2 subunit mutant mice. Neuron. 1996; 16:333–344. [PubMed: 8789948]

Li Y, Erzurumlu RS, Chen C, Jhaveri S, Tonegawa S. Whisker-related neuronal patterns fail to develop in the brainstem trigeminal nuclei of NMDAR1 knockout mice. Cell. 1994; 76:427–437. [PubMed: 8313466]

Lo FS, Guido W, Erzurumlu RS. Electrophysiological properties and synaptic responses of cells in the trigeminal principal sensory nucleus of postnatal rats. J Neurophysiol. 1999; 82:2765–2775. [PubMed: 10561443]

Luthi A, McCormick DA. H-current: properies of a neuronal and network pacemaker. Neuron. 1998; 21:9–12. [PubMed: 9697847]

Ma PM. The barrelettes-architectonic vibrissal representations in the brainstem trigeminal complex of the mouse. I. Normal structural organization. J Comp Neurol. 1991; 309:161–199. [PubMed: 1715890]

Ma PM. Barrellettes: architectonic vibrissal representations in the brainstem trigeminal complex of the mouse. II. Normal postnatal development. J Comp Neurol. 1993; 327:376–397. [PubMed: 8440772]

Ma PM, Woolsey TA. Cytoarchitectonic correlates of the vibrissae in the medullary trigeminal complex of the mouse. Brain Res. 1984; 306:374–379. [PubMed: 6205721]

McCormick DA, Prince DA. Postnatal development of electrophysiological properties of rat cerebral cortical pyramidal neurons. J Physiol (Lond). 1987; 393:743–762. [PubMed: 2895811]

MacLeod N, Turner C, Edgar J. Properties of developing lateral geniculate neurons in the mouse. Int J Dev Neurosci. 1997; 15:205–224. [PubMed: 9178039]

Martin-Caraballo M, Greer JJ. Electrophysiological properties of rat phrenic motoneurons during perinatal development. J Neurophysiol. 1999; 81:1365–1378. [PubMed: 10085362]

Molnar LR, Thayne KA, Fleming WW, Taylor DA. The role of the sodium pump in the developmental regulation of membrane electrical properties of cerebellar Purkinje neurons of the rat. Brain Res Dev Brain Res. 1999; 112:287–291.

Nasution ID, Shigenaga Y. Ascending and descending internuclear projections within the trigeminal sensory nuclear complex. Brain Res. 1987; 425:234–247. [PubMed: 2827843]

Neher E. Correction for liquid junction potentials in patch clamp experiments. Methods Enzymol. 1992; 207:123–131. [PubMed: 1528115]

Nunez-Abades PA, Speielmann JM, Barrionuevo G, Cameron WE. In vitro electrophysiology of developing genioglossal motoneurons in the rat. J Neurophysiol. 1993; 70:1401–1411. [PubMed: 8283205]

O'Leary DDM, Ruff NL, Dyck RH. Development, critical period plasticity, and adult reorganizations of mammalian somatosensory systems. Curr Opin Neurobiol. 1994; 4:535–544. [PubMed: 7812142]

Perez Velazquez JL, Carlen PL. Development of firing patterns and electrical properties in neurons of the rat ventrobasal thalamus. Brain Res Dev Brain Res. 1996; 91:164–170.

Pirchio M, Turner JP, Williams SR, Asprodini E, Crunelli V. Postnatal development of membrane properties and δ oscillations in thalamocortical neurons of the cat dorsal lateral geniculate nucleus. J Neurosci. 1997; 17:5428–5444. [PubMed: 9204926]

Ramoa AS, McCormick DA. Developmental changes in electrophysiological properties of LGNd neurons during reorganization of retinogeniculate connections. J Neurosci. 1994a; 14:2089–2097. [PubMed: 8158259]

Ramoa AS, McCoRMICK DA. Enhanced activation of NMDA receptor at the immature retinogeniculate synapse. J Neurosci. 1994b; 14:2098–2105. [PubMed: 7908957]

Reinagel P, Godwin D, Sherman SM, Koch C. Encoding of visual information by LGN bursts. J Neurophysiol. 1999; 81:2558–2569. [PubMed: 10322089]

Rothe T, Juttner R, Bahring R, Grantyn R. Ion conductances related to development of repetitive firing in mouse retinal ganglion neurons in situ. J Neurobiol. 1999; 38:191–206. [PubMed: 10022566]

Sandler VM, Puil E, Schwarz DWF. Intrinsic response properties of bursting neurons in the nucleus principalis tragemini of the gerbil. Neuroscience. 1998; 83:891–904. [PubMed: 9483572]

Soltesz I, Lightowler S, Leresche N, Jassik-Gerschenfeld D, Pollard CE, Crunelli V. Two inward currents and the transformation of low-frequency oscillations of rat and cat thalamo-cortical cells. J Physiol (Lond). 1991; 441:175–197. [PubMed: 1667794]

Spigelman I, Zhang L, Carlen PL. Patch-clamp study of postnatal development of CA1 neurons in rat hippocampal slices: membrane excitability and $K^+$ currents. J Neurophysiol. 1992; 68:55–69. [PubMed: 1517828]

Steriade M, McCormick DA, Sejnowski TJ. Thalamocortical oscillations in the sleeping and aroused brain. Science. 1993; 262:679–685. [PubMed: 8235588]

Tennigkeit F, Schwarz DW, Puil E. Postnatal development of signal generation in auditory thalamic neurons. Brain Res Dev Brain Res. 1998; 109:255–263.

Tsuzuki S, Yoshida S, Yamamoto T, Oka H. Developmental changes in the electrophysiological properties of neonatal rat oculomotor neurons studied in vitro. Neurosci Res. 1995; 23:389–397. [PubMed: 8602279]

Van der Loos H. Barreloids in mouse somatosensory thalamus. Neurosci Lett. 1976; 2:1–6. [PubMed: 19604804]

Van der Loos H, Woolsey TA. Somatosensory cortex: structural alterations following early injury to sense organs. Science. 1973; 179:395–398. [PubMed: 4682966]

Viana F, Bayliss DA, Berger AJ. Postnatal changes in rat hypoglossal motoneuron membrane properties. Neuroscience. 1994; 59:131–148. [PubMed: 8190264]

Vincent A, Tell F. Postnatal development of rat nucleus tractus solitarius neurons: morphological and electrophysiological evidence. Neuroscience. 1999; 93:293–305. [PubMed: 10430493]

Wang GY, Ratto GM, Bisti S, Chalupa LM. Functional development of intrinsic properties in ganglion cells of the mammalian retina. J Neurophysiol. 1997; 78:2895–2903. [PubMed: 9405510]

Warren RA, Jones EG. Maturation of neuronal form and function in a mouse thalamo-cortical circuit. J Neurosci. 1997; 17:277–295. [PubMed: 8987755]

Wong-Riley MT, Welt C. Histochemical changes in cytochrome oxidase of cortical barrels after vibrissal removal in neonatal and adult mice. Proc Natl Acad Sci USA. 1980; 77:2333–2337. [PubMed: 6246540]

Woolsey, TA. Peripheral alteration and somatosensory development. In: Coleman, EJ., editor. Development of Sensory Systems in Mammals. New York: Wiley; 1990. p. 461-516.

Yip VS, Zhang WP, Woolsey TA, Lowry OH. Quantitative histochemical and microchemical changes in the adult mouse CNS after section of the intraorbital and optic nerves. Brain Res. 1987; 406:157–170. [PubMed: 3032355]

Zhou FM, Hablitz JJ. Postnatal development of membrane properties of layer I neurons in rat neocortex. J Neurosci. 1996; 16:1131–1139. [PubMed: 8558242]

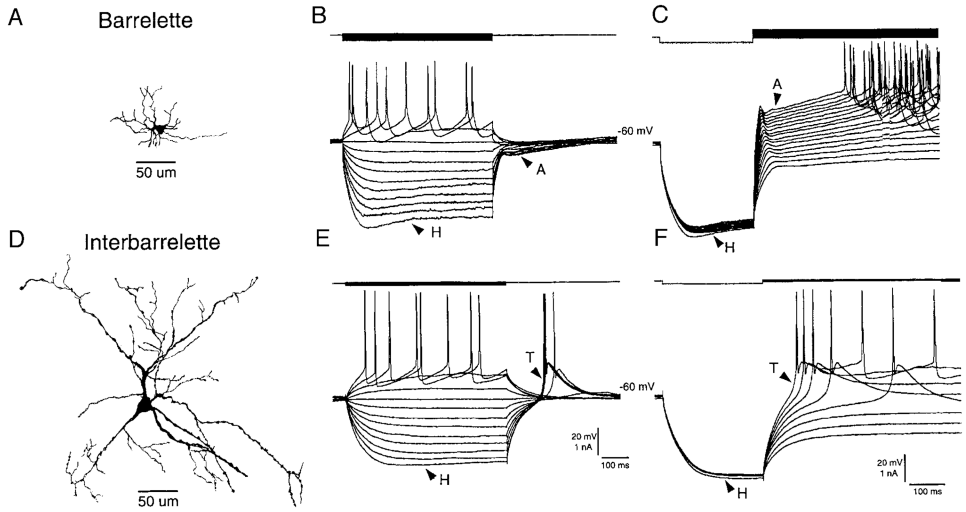


**Fig. 1.**

Classification of neurons in principal sensory nucleus of the trigeminal nerve (PrV). *A*: an example of a biocytin-labeled barrelette cell. *B* and *C*: voltage responses of the barrelette neuron in *A* to intracellular current injection. *Top*: current pulses; *bottom*: voltage responses. *B*: strong hyperpolarization activates a mixed cation conductance (H), which produces a depolarizing "sag" in the response. Note the long hyperpolarizing tail (A) on cessation of the hyperpolarizing current pulse. This response reflects the activation of an A-type conductance. *C*: activation of A-type conductance is also evident at different depolarizing levels following membrane hyperpolarization. Note the hyperpolarizing notch (A) that delays the generation of action potentials. *D*: an example of a biocytin-labeled interbarrelette cell. *E* and *F*: voltage responses of the interbarrelette neuron in *D* to intracellular current injection. *E*: the interbarrelette cell also shows a depolarizing sag (H) during strong hyperpolarization. On termination of the hyperpolarizing pulses, the passive repolarization of the membrane triggers a rebound low-threshold $Ca^{2+}$ spike (T) that contains a burst of action potentials riding its peak. *F*: low-threshold $Ca^{2+}$ spikes are also triggered by membrane depolarization from hyperpolarized levels. Barrelette neurons possess prominent H- and A-type conductances. Whereas interbarrelette neurons, in addition to H, also possess a prominent low-threshold $Ca^{2+}$ conductance.

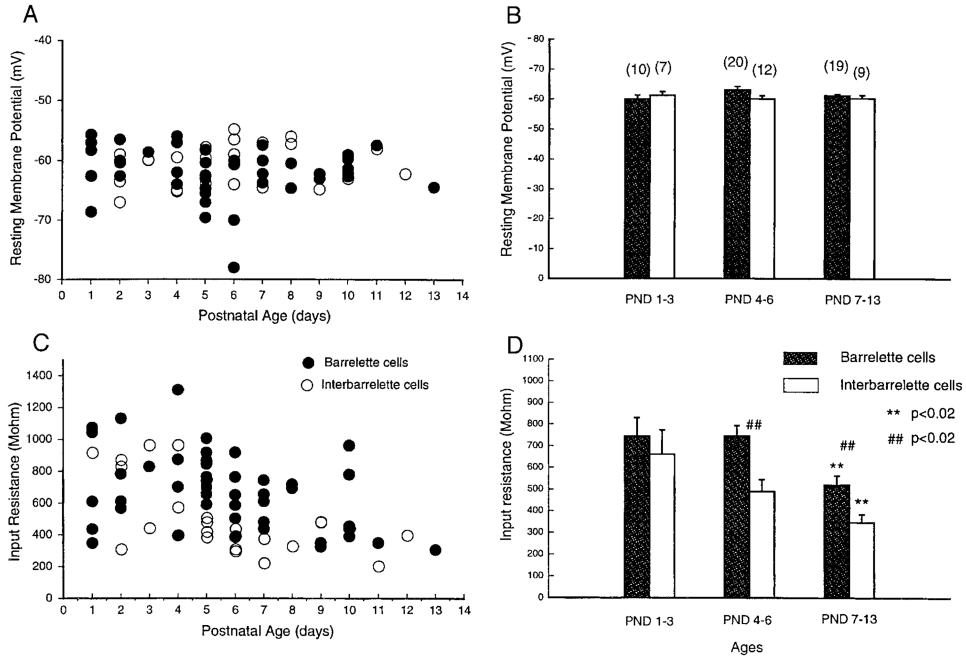


**Fig. 2.**

Developmental changes in passive membrane properties of barrelette and interbarrelette cells. *A*: scatter plot of resting membrane potentials against postnatal ages for the 2 types of cells. ●, barrelette cells. ○, interbarrelette cells. *B*: averaged resting potentials at different ages for barrelette cells ( ▩) and interbarrelette cells (□). Bar: mean value. Error bar: SE. Number in parentheses: tested cell number. Note that there are no developmental changes in resting potentials ($P > 0.05$) for both cell types and no difference ($P > 0.05$) between the 2 types at all age groups. *C*: scatter plot of input resistances of the 2 types of cells suggests a decrease in input resistances with age. *D*: input resistances in both barrelette and interbarrelette cells are significantly smaller at postnatal days (PND) 7–13 than those at PND 1–3 ($P < 0.02$, **). Because the input resistance of interbarrelette cells declines faster than that of barrelette cells, the input resistance of the 2 types is significantly different ($P < 0.02$, ##) at PND 4–6 and PND 7–13.

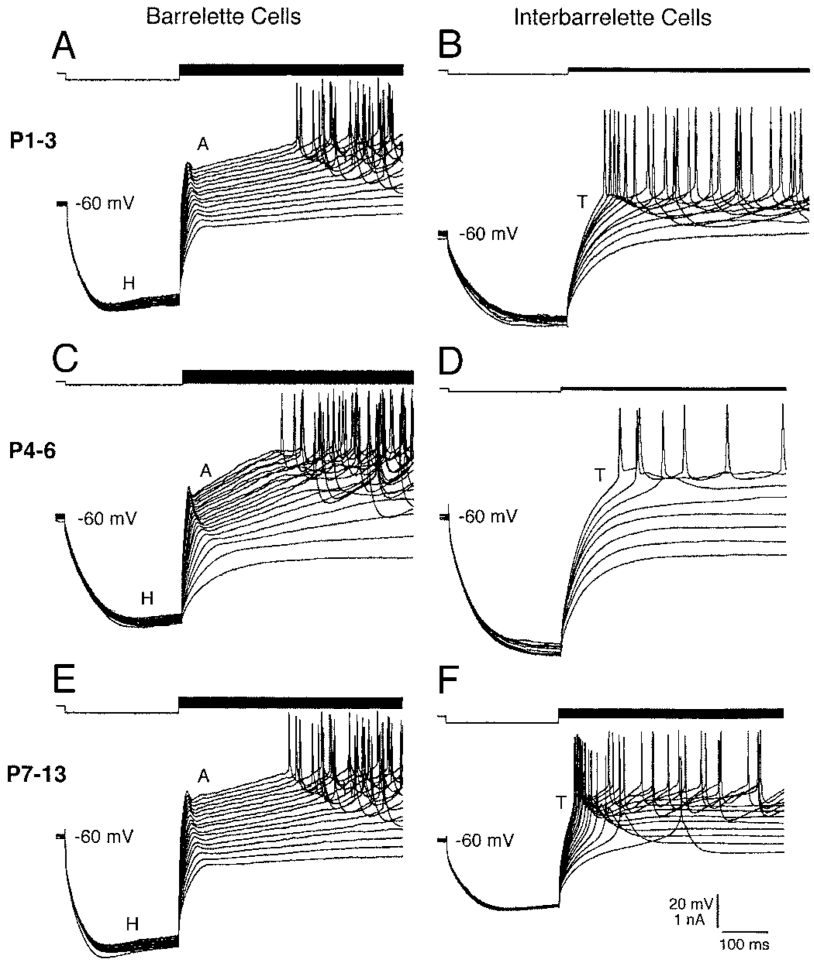


**Fig. 3.**

The presence of $I_A$, $I_T$, and $I_H$ at PND 1. *A, C*, and *E*: barrelette cells from PND1 to PND13 have both $I_A$ and $I_H$. $Na^+$ spikes remain unchanged during development. *B, D*, and *F*: interbarrelette cells from PHD1 to PND13 show $I_T$. Note that there is a trend to increase amplitude of low-threshold spikes (LTSs) with age.

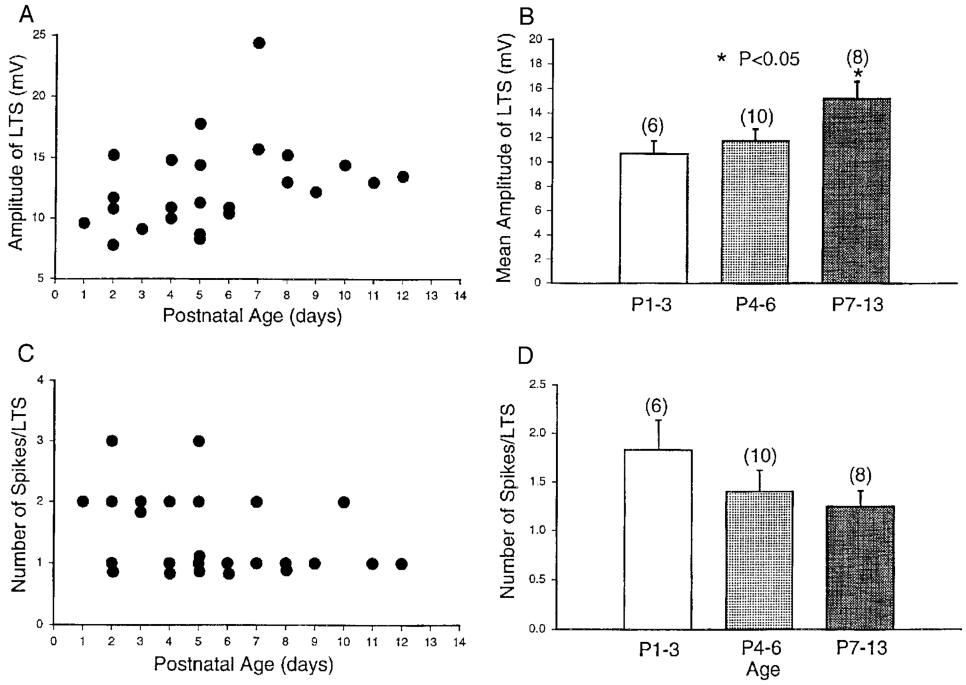


**Fig. 4.**

Developmental changes in $I_T$ of interbarrelette cells. *A*: scatter plot of LTS amplitudes suggests an increase in LTS amplitude with age. *B*: the averaged amplitude of LTS at PND 7–13 is significantly larger ($P < 0.05$) than that at PND 1–3. *C*: scatter plot of numbers of $Na^+$ spikes riding on LTS against postnatal ages. *D*: there seems to be a trend to decrease the number of spikes with age, but the difference is not statistically significant.

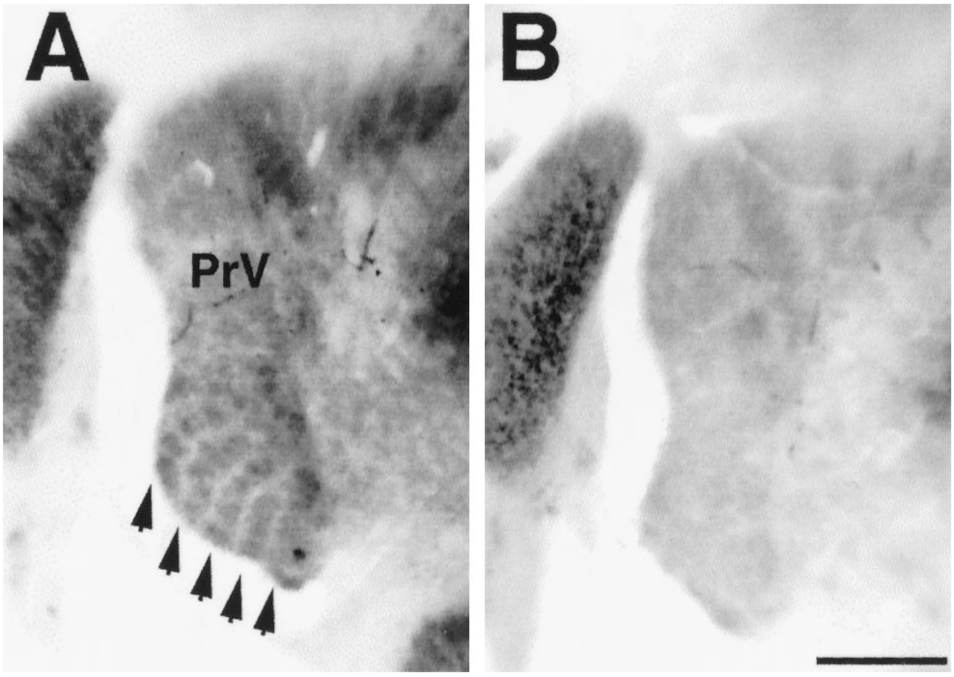


**Fig. 5.**

Denervation by infraorbital nerve section at birth abolishes bar-relettes in PrV. Cytochrome oxidase (CO)-stained sections through the PrV of a PND 5 rat pup that underwent unilateral infraorbital nerve section at birth. *A*: normal barrelette pattern in the PrV (↑) on the control side. *B*: abolished CO-positive barrelettes on the denervated side. The photograph of the experimental side shown in *B* was flipped to match the orientation of the nucleus to the control side. In both photomicrographs, dorsal is up and medial is to the left. Scale bar = 250 $\mu$m.

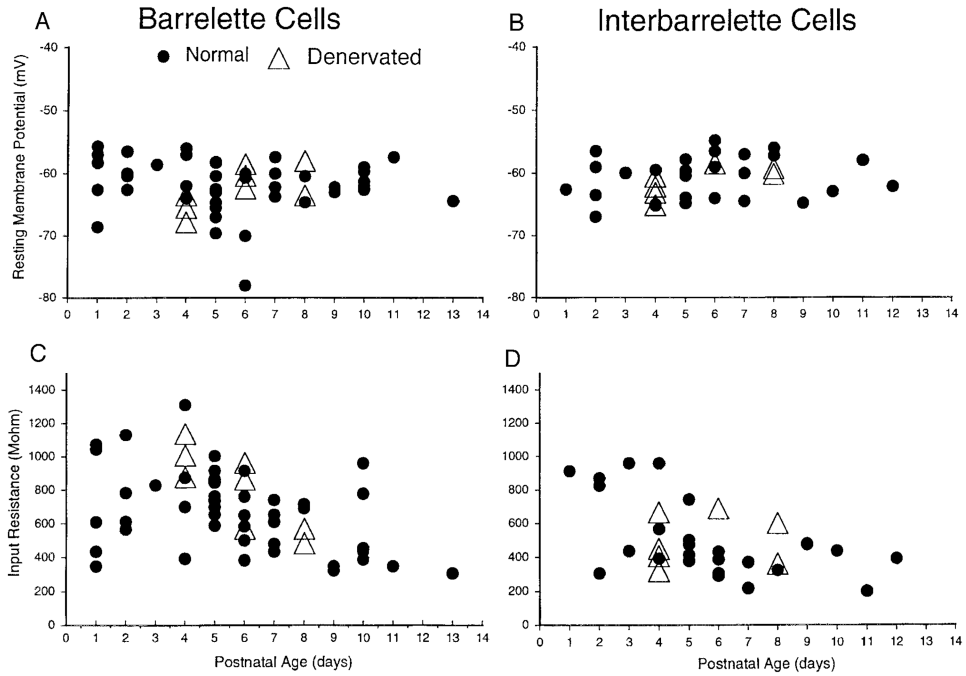


**Fig. 6.**

Denervation does not alter passive membrane properties of PrV neurons. Following infraorbital nerve section at birth, whole cell recordings are performed at PND 4–8. *A*: scatter plot of resting potentials for barrelette cells (●) and "barrelette" cells of denervated rats (Δ). *B*: scatter plot of resting potentials for interbarrelette cells and "interbarrelette" cells of denervated rats. *C*: scatter plot of input resistances for barrelette cells and "barrelette" cells of denervated rats. *D*: scatter plot of input resistances for interbarrelette cells and "interbarrelette" cells of denervated rats. Note that denervation does not change the resting potential and the decline in input resistance.

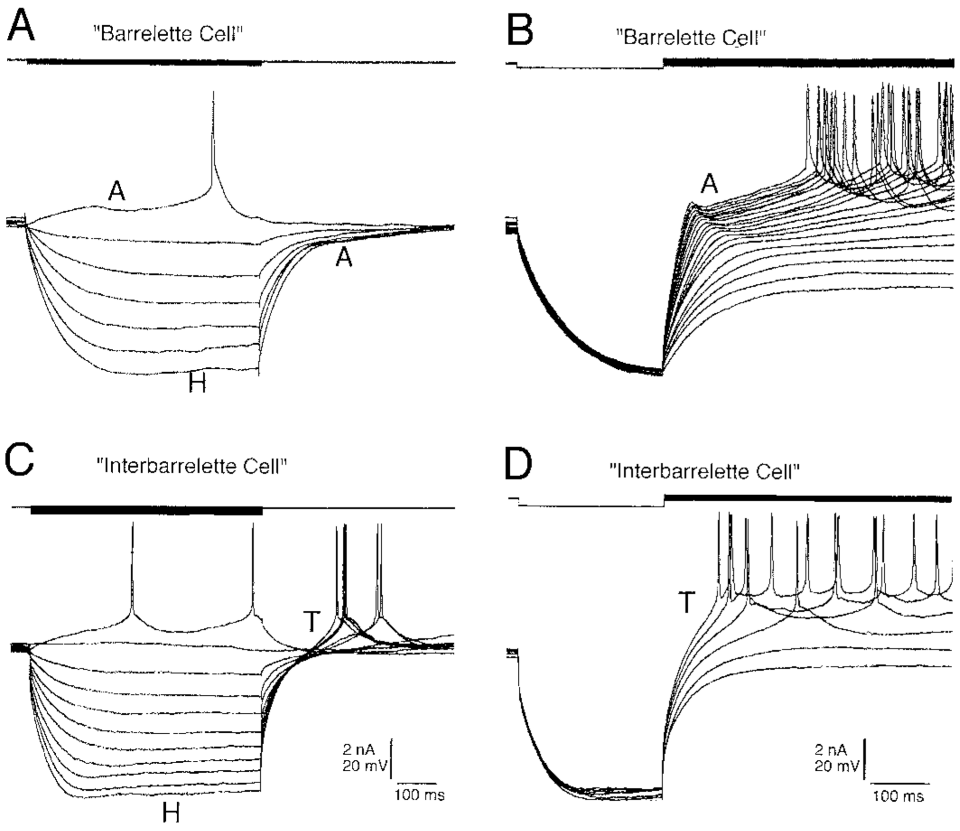


**Fig. 7.**

Denervation does not alter active conductances of PrV neurons. *A* and *B*: "barrelette" cells still show $I_A$ and $I_H$. *C* and *D*: "interbarrelette" cells exhibit $I_T$ and $I_H$.